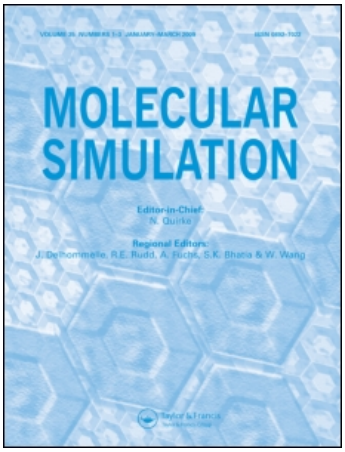

Molecular Simulation
Publication details, including instructions for authors and subscription information:
http://www.informaworld.com/smpp/title~content=t713644482

Comparisons of diffusive and viscous contributions to transport coefficients of light gases in single-walled carbon nanotubes

Suresh K. Bhatia[a]; Haibin Chen[b]; David S. Sholl[bc]
[a] Division of Chemical Engineering, The University of Queensland, Brisbane, Australia [b] Department of Chemical Engineering, Carnegie Mellon University, Pittsburgh, PA, USA [c] National Energy Technology Laboratory, Pittsburgh, PA, USA

To cite this Article Bhatia, Suresh K. , Chen, Haibin and Sholl, David S.(2005) 'Comparisons of diffusive and viscous contributions to transport coefficients of light gases in single-walled carbon nanotubes', Molecular Simulation, 31: 9, 643 — 649
To link to this Article: DOI: 10.1080/00268970500108403
URL: http://dx.doi.org/10.1080/00268970500108403

Molecular Simulation, Vol. 31, No. 9, August 2005, 643–649

Taylor & Francis
Taylor & Francis Group

Comparisons of diffusive and viscous contributions to transport coefficients of light gases in single-walled carbon nanotubes

SURESH K. BHATIA†*, HAIBIN CHEN‡ and DAVID S. SHOLL‡,¶

†Division of Chemical Engineering, The University of Queensland, Brisbane, Qld 4072, Australia
‡Department of Chemical Engineering, Carnegie Mellon University, Pittsburgh, PA 15213, USA
¶National Energy Technology Laboratory, Pittsburgh, PA 15236, USA

(Received November 2004; in final form January 2005)

We examine here the relative importance of different contributions to transport of light gases in single walled carbon nanotubes, using methane and hydrogen as examples. Transport coefficients at 298 K are determined using molecular dynamics simulation with atomistic models of the nanotube wall, from which the diffusive and viscous contributions are resolved using a recent approach that provides an explicit expression for the latter. We also exploit an exact theory for the transport of Lennard-Jones fluids at low density considering diffuse reflection at the tube wall, thereby permitting the estimation of Maxwell coefficients for the wall reflection. It is found that reflection from the carbon nanotube wall is nearly specular, as a result of which slip flow dominates, and the viscous contribution is small in comparison, even for a tube as large as 8.1 nm in diameter. The reflection coefficient for hydrogen is 3–6 times as large as that for methane in tubes of 1.36 nm diameter, indicating less specular reflection for hydrogen and greater sensitivity to atomic detail of the surface. This reconciles results showing that transport coefficients for hydrogen and methane, obtained in simulation, are comparable in tubes of this size. With increase in adsorbate density, the reflection coefficient increases, suggesting that adsorbate interactions near the wall serve to roughen the local potential energy landscape perceived by fluid molecules.

Keywords: Transport coefficients; Single-walled carbon nanotubes; Lennard-Jones fluids; Maxwell coefficients

1. Introduction

Many industrial processes exploit the properties of small molecules adsorbed inside micropores. Well known examples include catalysis performed using microporous materials and separations performed using either packed beds or membranes of microporous materials [1–3]. In many instances, particularly in membrane-based processes, the transport properties of adsorbed species are of vital importance. For this reason, any material that is found to have transport properties that are radically different from those of other materials is a strong candidate material for application in innovative processes. One material that falls into this class is single-walled carbon nanotubes (SWNTS). A number of recent modeling studies have indicated that molecular transport rates inside SWNTs are orders of magnitude higher than in all other microporous materials [4–7]. The very high transport rates observed in these studies arise from the very smooth internal surfaces that exist inside SWNTs, which give rise to near-specular reflection of molecules when they contact the nanotube walls. For flat surfaces the effect of surface morphology on the nature of the reflection, spanning a range between near specular to near diffuse reflection, has recently been studied through simulation of molecule wall collisions [8]. While the results are consistent with near specular reflection for graphitic surfaces, where the covalently bonded carbon atoms are relatively closely spaced compared to the length scale of the fluid–solid interaction, the quantitative application to carbon nanotubes requires further study, due to the strong effect of curvature. Some work along these lines has been reported previously by Sokhan *et al.* [7], who investigate molecule wall collisions in nanotubes with the aim of suggesting boundary conditions for use in molecular dynamics studies where a one-dimensional potential is employed in the nanotube.

The simulation studies of SWNTs mentioned above have focused on nanotubes with diameters of 1–2 nm. These pore diameters were chosen because many synthesis methods that create bundles of nanotubes give pores of this size [9]. Recently, the first experimental

*Corresponding author. Email: sureshb@cheque.uq.edu.au

Molecular Simulation
ISSN 0892-7022 print/ISSN 1029-0435 online © 2005 Taylor & Francis Group Ltd
http://www.tandf.co.uk/journals
DOI: 10.1080/00268970500108403

realization of a membrane comprised of carbon nanotubes was described by Hinds *et al.* [10]. In these experiments, individual nanotubes spanned an impermeable polymer matrix, allowing transport of both gases and liquids. The diameter of the nanotubes in these experiments was $\sim$7.5 nm, so these pores were significantly larger than those examined in previous simulation studies.

The net transport of a single adsorbed component inside a SWNT can be defined through the so-called corrected diffusivity, D_O, which relates a net gradient in the adsorbed species' chemical potential to the net flux, j, by [11]

$$j = -\hat{\rho}\frac{D_O(\hat{\rho})}{\mathrm{RT}}\frac{\mathrm{d}\mu}{\mathrm{d}z}, \tag{1}$$

here, $\hat{\rho}$ is the adsorbate density in the pore. For a single adsorbed component, the corrected diffusivity is identical to the Maxwell-Stefan diffusivity [12]. Corrected diffusivities can be computed from atomically-detailed models of microporous materials using equilibrium molecular dynamics (EMD) [13–15], non-equilibrium molecular dynamics (NEMD) [13,15], or dual control volume grand canonical molecular dynamics (DCV-GCMD) [13,15]. These simulation methods have previously been applied to a range of microporous materials, including SWNTs [4], zeolites [13] and more recently, metal organic framework materials [16].

While MD can be used to directly determine D_O for particular systems of interest, these calculations are time-consuming. More importantly, MD simulations must be performed independently for each state point and material of interest. This property makes it challenging to systematically study the transport properties of adsorbed species in SWNTs as the nanotube diameter varies over the broad range of diameters observed in different experiments. Clearly, it would be useful to complement MD simulations of these systems with a theoretical description that can describe the different physical contributions to net transport in SWNTs in a way that can be used to assess a range of pore sizes. The aim of this paper is to demonstrate an approach to this problem.

To develop a theory for transport in SWNTs that is complementary to MD simulations, we write the corrected diffusivity as a contribution of two terms [17]

$$D_O(\hat{\rho}) = D_{\mathrm{diff}}(\hat{\rho}) + D_{\mathrm{vis}}(\hat{\rho}), \tag{2}$$

where the diffusive contribution, $D_{\mathrm{diff}}(\hat{\rho})$, arises from wall–fluid interactions, and the viscous contribution, $D_{\mathrm{vis}}(\hat{\rho})$, arises from fluid–fluid interactions. By using theoretical models for each of these two contributions, the affect of pore size can be examined. This approach is also useful for interpreting MD results since it allows the relative size of the diffusive and viscous contributions to transport to be quantified.

Analysis of the viscous contribution to transport in pores has a long history, beginning with the pioneering work of Knudsen and of Smoluchowski [18], with several subsequent more elaborate treatments, such as that of Pollard and Present [19]. Much of this work has considered pores much larger than molecular diameters where details of wall-adsorbate interactions can be neglected. In recent years, a new approach to tackle the challenging problem of characterizing the viscous part of $D_{\mathrm{vis}}(\hat{\rho})$ in cases where wall-adsorbate interactions are significant has been suggested [17,20,21], motivated by the suggestion of Bitsanis *et al.* [22] that the Navier–Stokes equation may be integrated over the pore cross-section with a position-dependent viscosity, evaluated at a locally averaged density. While Bitsanis *et al.* considered constant pressure gradient over the pore cross-section, our recent work [17,20,21] has instead considered constant chemical potential over the cross section. The latter is based on the observation that density profiles from NEMD match those obtained during grand canonical Monte Carlo (GCMC) simulation [17,20,21,23]. In the present work we have followed this more recent approach.

The paper is organized as follows. Section 2 describes the theoretical and simulation methods used to assess diffusive and viscous contributions to transport in SWNTs. An analysis of the transport properties of CH_4 and H_2 as single-components inside (10,10) SWNTs is given in section 3. Section 4 extends this analysis by considering SWNTs with larger diameters. Our results are summarized and some directions for future work are identified in section 5.

2. Methods

2.1. Atomistic models of CH_4 and H_2 in SWNTs

Atomically detailed models of CH_4 and H_2 adsorption inside defect-free SWNTs were adopted from our earlier work [4]. Briefly, both adsorbing species are represented as Lennard-Jones spheres, and interactions between adsorbed molecules and SWNTs are represented using Lennard-Jones interactions between each molecule and C atom in the SWNT. The SWNTs were assumed to be rigid, an approach whose validity has been carefully discussed by Sokhan *et al.* [7]. When performing MD simulations, no scattering of particle trajectories was introduced during wall–fluid collisions aside from that arising from the intrinsic corrugation of the wall–fluid potential. The details of the GCMC and equilibrium MD calculations used in our analysis below have been given previously [4].

2.2. Viscous contributions to transport

As indicated above, we have followed the recent approach of Bhatia *et al.* [17,20,21,23] for evaluating the viscous contribution to the net transport for each adsorbate-pore pair of interest. This method gives

$$D_{\mathrm{vis}}(\hat{\rho}) = \frac{2k_BT}{\hat{\rho}r_p^2}\int_o^{r_o}\frac{\mathrm{d}r}{r\eta(\bar{\rho}(r))}\left(\int_o^r r'\rho(r')\,\mathrm{d}r'\right)^2 \tag{3}$$

where $\rho(r)$ is the radial density profile of the adsorbate. Since cross-sectional equilibrium is attained during transport as discussed above, these density profiles can be equated with the equilibrium profiles computed from our GCMC simulations. In this formulation, $\eta(\bar{\rho})$ represents a (non) local viscosity evaluated at a density locally averaged over a sphere of radius $\sigma_{ff}/2$, where σ_{ff} is the fluid molecular diameter, taken as its LJ diameter. Thus,

$$\bar{\rho}(\mathbf{r}) = \frac{6}{\pi\sigma_f^3}\int_{|r'|<\sigma_f/2} \rho(\mathbf{r}+\mathbf{r}')\,\mathrm{d}\mathbf{r}' \tag{4}$$

Once $\bar{\rho}$ has been calculated in this way, the viscosity is evaluated using the empirical correlation of Chung *et al.* [24]. Other correlations more specifically developed for the viscosity of LJ fluids also exist [25,26], but have not been widely tested and were found to be highly inaccurate for hydrogen in our work. Hence, the choice of the Chung *et al.* correlation was made in this study. Alternately, bulk simulations could be used to develop viscosity–density correlations for each chosen fluid, for use in equation (3). However, in the present study, this was not considered necessary, given the relative insignificance of viscous transport, which will be subsequently demonstrated.

2.3. Maxwell coefficients for diffusive transport

The diffusive contribution to net transport in equation (2), $D_{\mathrm{diff}}(\hat{\rho})$, arises from the interactions between adsorbed molecules and the pore wall. For particles that undergo diffuse reflection each time they collide with the pore wall of a cylindrical pore, the diffusive contribution in the low-density limit, $\mathrm{D}_{\mathrm{diff}}^{\mathrm{DR}}(\hat{\rho}=0)$, can be expressed analytically, following the oscillator model of Bhatia and co-workers [17,27]. If $\phi_{\mathrm{fs}}(r)$ is the radial potential energy of the fluid–solid interaction in the pore, then

$$D_{\mathrm{diff}}^{\mathrm{DR}}(\hat{\rho}=0) = \frac{2}{\pi m Q}\int_0^\infty e^{-\beta\phi_{\mathrm{fs}}(r)}\,\mathrm{d}r \int_0^\infty e^{-\beta p_r^2/2m}\,\mathrm{d}p_r \times \int_0^\infty e^{-\beta p_\theta^2/2mr^2}\,\mathrm{d}p_\theta \int_{r_{c0}(r,p_r,p_\theta)}^{r_{c1}(r,p_r,p_\theta)} \frac{\mathrm{d}r'}{p_r(r',r,p_r,p_\theta)}, \tag{5}$$

where $Q = \int_0^\infty r e^{-\beta\phi_{\mathrm{fs}}(r)}\,\mathrm{d}r$, and

$$p_r(r',r,p_r,p_\theta) = \left\{2m[\phi_{\mathrm{fs}}(r)-\phi_{\mathrm{fs}}(r')] + p_r^2(r) + \frac{p_\theta^2}{r^2}\left(1-\frac{r^2}{r'^2}\right)\right\}^{1/2}, \tag{6}$$

Here, $p_r(r',r,p_r,p_\theta)$ is the radial momentum at position r' for a particle having radial momentum p_r at position r and angular momentum p_θ (a constant of the motion, since there are no tangential forces in the case of a one dimensional potential). Further, $r_{c0}(r,p_r,p_\theta)$ and $r_{c1}(r,p_r,p_\theta)$ are the values of r' corresponding to the limits of the radial motion, obtained from the solution of

$$p_r(r',r,p_r,p_\theta) = 0. \tag{7}$$

It is important to note that in our atomistic simulations, the fluid solid potential is a function of both r and θ, z because this potential is calculated based on the positions of each atom in the SWNT. For SWNT's the corrugations in this potential at fixed r as θ and z are varied are very small [14], so that we can describe ϕ_{fs} as $\phi_{\mathrm{fs}}(r)$ above without loss of accuracy.

The above theory is exact for the case of diffuse reflection from the pore wall. This has been verified over a wide range of pore sizes by molecular dynamics simulation studies for methane diffusion in silica pores [17,27], and in carbon slit pores [23]. More recent work with other adsorptives has provided further confirmation [28].

The result in equation (5) is not appropriate for describing adsorbate diffusion in SWNTs because it assumes diffuse reflection at the pore walls. That is, each particle is taken to completely thermalize and lose all memory of its velocity during each collision with the wall. MD simulations by several groups have shown that the situation for small molecules inside SWNTs is almost opposite to this description; observed wall collisions are almost specular, so many consecutive collisions are required before an adsorbate's velocity becomes decorrelated with its initial velocity. One useful framework for characterizing this effect is to introduce the Maxwell coefficient, α, associated with collision with the wall [18]. This approach assumes that a fraction α of all collisions result in diffuse reflection while all remaining collisions are specular. It is possible to generalize equation (5) to systems with $\alpha < 1$ which gives [18,23]

$$D_{\mathrm{diff}}^{\alpha}(\hat{\rho}=0) = \frac{(2-\alpha)}{\alpha} D_{\mathrm{diff}}^{\mathrm{DR}}(\hat{\rho}=0). \tag{8}$$

3. Transport properties of (10,10) SWNTs

In this section, we consider the transport of CH_4 and H_2 as single components in (10,10) SWNTs at room temperature. The density-dependent corrected transport diffusivities, $D_O(\hat{\rho})$, for these two species have been calculated previously using EMD [4]. We can reinterpret these diffusivities via equation (2) by writing

$$D_O(\hat{\rho}) = \frac{(2-\alpha)}{\alpha} D_{\mathrm{diff}}^{\mathrm{DR}}(\hat{\rho}=0) + D_{\mathrm{vis}}(\hat{\rho}), \tag{9}$$

where $D_{\mathrm{vis}}(\hat{\rho})$ and $D_{\mathrm{diff}}^{\mathrm{DR}}(\hat{\rho}=0)$ are calculated using equations (3) and (5), respectively. That is, we can use the diffusivities measured using MD to determine the Maxwell coefficients, α. As we will show below, the resulting Maxwell coefficients are weakly dependent on density, that is, $\alpha = \alpha(\hat{\rho})$. This result can be considered as describing the influence of fluid–fluid interactions on the character of wall–fluid collisions.

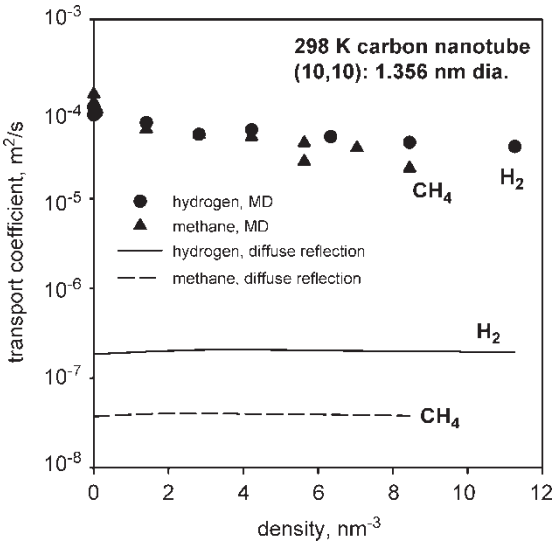

Figure 1. Corrected diffusion coefficients for CH_4 and H_2 adsorbed as single components in (10,10) SWNTs. Filled symbols represent results from EMD simulations [6]. Curves represent the predictions of the right hand side of equation (9) assuming diffuse reflections ($\alpha = 1$).

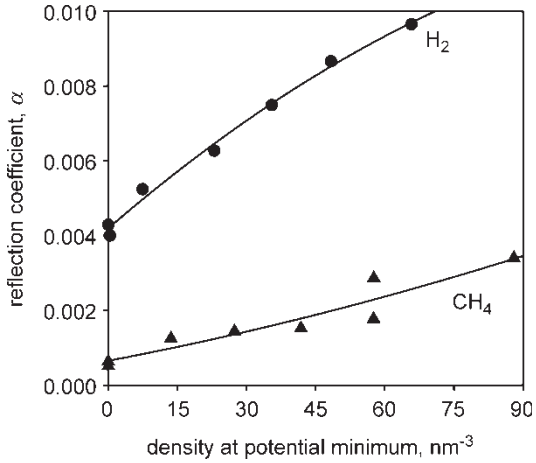

Figure 2. Density dependent Maxwell coefficients for CH_4 and H_2 in (10,10) SWNTs calculated as described in the text.

The corrected diffusivities obtained from EMD simulations for CH_4 and H_2 in (10,10) SWNTs are shown in figure 1. The density of each adsorbate inside the nanotube is reported by treating the pore as a cylinder with diameter 1.356 nm. As has been discussed previously, the magnitude of the diffusivities is very large [4]. These diffusivities are similar in magnitude to typical diffusion coefficients in gases, and orders of magnitude larger than diffusion coefficients in other microporous materials such as zeolites or polymers. Figure 1 also shows the result predicted by the right hand side of equation (9) in the limit of diffuse reflection, that is $\alpha = 1$. For both species, this prediction is orders of magnitude smaller than the actual diffusion coefficient, giving a clear indication of the strong deviations from diffuse reflection that occur in these materials. MD simulations [29] of gas transport in SWNTs in which diffusing atoms were thermalized with the wall on collision, thereby invoking diffuse reflections for fluid–wall collisions, following the thermal scattering algorithm of MacElroy and Boyle [30], have given diffusion coefficients quite similar to those predicted using $\alpha = 1$ in figure 1. The large deviation of the results based on diffuse reflection demonstrates the importance of properly treating the fluid–wall collision. A further interesting feature of figure 1 is that in the actual nanotube the diffusivities of methane and hydrogen are comparable, although under conditions of diffuse reflection hydrogen diffuses faster by a factor of about 5, suggesting that the latter is more diffusely reflected.

The density-dependent Maxwell coefficients for CH_4 and H_2 determined using equation (9) are shown in figure 2. In this figure the density is reported using the local density at the minimum of the radial potential as computed using GCMC, since this provides a useful description of the local environment in which the diffusing molecules exist. As should be expected from figure 1, the Maxwell coefficients are very close to zero, indicating that typical wall–fluid collisions are extremely close to being purely specular.

For CH_4, the Maxwell coefficient ranges from 0.0006 at the lowest densities to 0.0034 at the highest densities were examined. These values are consistent with those determined by Sokhan *et al.* using direct simulation of fluid–wall collisions [7]. The values of α for H_2 in the (10,10) SWNT are larger than those for methane by a factor of 3–6, reconciling the above observation that hydrogen is more diffusely reflected. This observation can be understood by considering the smaller size of H_2 relative to CH_4, which results in the roughness of the energy landscape near the nanotube wall being larger for H_2 than for CH_4. The impact of this effect on the relative diffusion coefficients of H_2 and CH_4 has been discussed previously based on MD simulations [4].

For both species, the Maxwell coefficient increases as the adsorbate density in the pore density increases. The fact that the Maxwell coefficient changes with adsorbate density arises from the indirect impact of fluid–fluid interactions on the character of wall–fluid collisions. Our results indicate that increasing fluid densities make the wall–fluid collisions slightly less specular, that is, these interactions effectively "roughen" the surface. This outcome is not surprising, since the presence of fluid–fluid interactions offers additional channels for energy transfer during wall–fluid collisions.

It may be noted that while we have based our measure of the degree of diffuse reflection by the value of the Maxwell coefficient α, following the classical model [18] that a fraction α of the reflections are diffuse and the remainder are specular, an alternate approach that considers each collision to contain both diffuse and specular components may also be employed. When this is done, the factor $(2 - \alpha)/\alpha$ in equation (8) requires modification, as demonstrated by Arya *et al.* [31] with the help of molecular dynamics simulations in which incident and reflected velocity distributions were used to compute

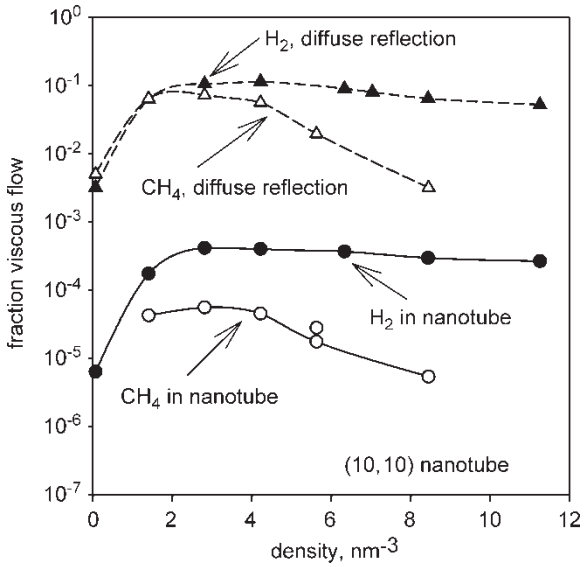

Figure 3. The fraction of the corrected diffusion coefficient arising from viscous contributions for CH_4 and H_2 in (10,10) SWNTs using diffusion coefficients determined from MD simulations (circles and solid curves) and assuming pure diffuse reflection (triangles and dashed curves). Curves are to guide the eye.

the value of α. In reality, since each collision is individually influenced by the local morphology of the surface the value of the coefficient α will not be uniform, and must represent an effective value. Consequently, both approaches are essentially effective representations and when velocity distributions are interpreted by either approach the appropriate factor will produce the correct transport coefficient in a consistent simulation. Thus, there is no obvious choice regarding the definition of α.

Figure 3 shows the fraction of the total diffusion coefficient that arises from viscous contributions for H_2 and CH_4 inside (10,10) SWNTs, that is, $D_{\rm vis}(\hat{\rho})/D_O(\hat{\rho})$. Under all conditions, this fraction is very small. That is, transport in these pores is dominated by contributions arising from wall–fluid collisions rather than from viscous effects. One implication of this observation is that our analysis above is a highly accurate means to determine the Maxwell coefficients in this system, since in using equation (9) our representation of $D^{\rm DR}_{\rm diff}(\hat{\rho}=0)$ is exact and any inaccuracies in our estimation of the viscous contributions will be insignificant. Figure 3 also shows how important the viscous contributions are if one assumes diffuse reflections for wall–fluid collisions, that is $D_{\rm vis}(\hat{\rho})/D^{\rm DR}_{\rm diff}(\hat{\rho}=0)$. In this limit viscous contributions are not negligible, particularly for H_2, where under many conditions the viscous contributions account for approximately 10% of the total transport coefficient.

4. Transport properties of larger diameter nanotubes

In this section, we use the theoretical framework described above to predict the transport properties of CH_4 and H_2 in (40,40) and (60,60) SWNTs at room temperature. These two materials have pore diameters (atom to atom) of 5.424 and 8.136 nm, respectively. These pore diameters are similar to the materials used as membranes in the recent experiments of Hinds *et al.* [10]. The main aim of our calculations is to estimate the relative importance of viscous contributions to net transport in these pores.

To use equation (9) predictively, we must estimate the Maxwell coefficients for the materials of interest. For both (40,40) and (60,60) SWNTs, we assume that the Maxwell coefficient is similar to that of planar graphite. Sokhan *et al.* previously reported that $\alpha = 0.013$ for CH_4 on planar graphite [32], so we adopted this value. As noted by Sokhan *et al.* [7], this Maxwell coefficient is considerably larger than the coefficient for narrow nanotubes, although it is still close to zero. No previous values of α for H_2 on planar graphite have been reported. We noted above that in (10,10) nanotubes the Maxwell coefficient for H_2 was 3–6 times

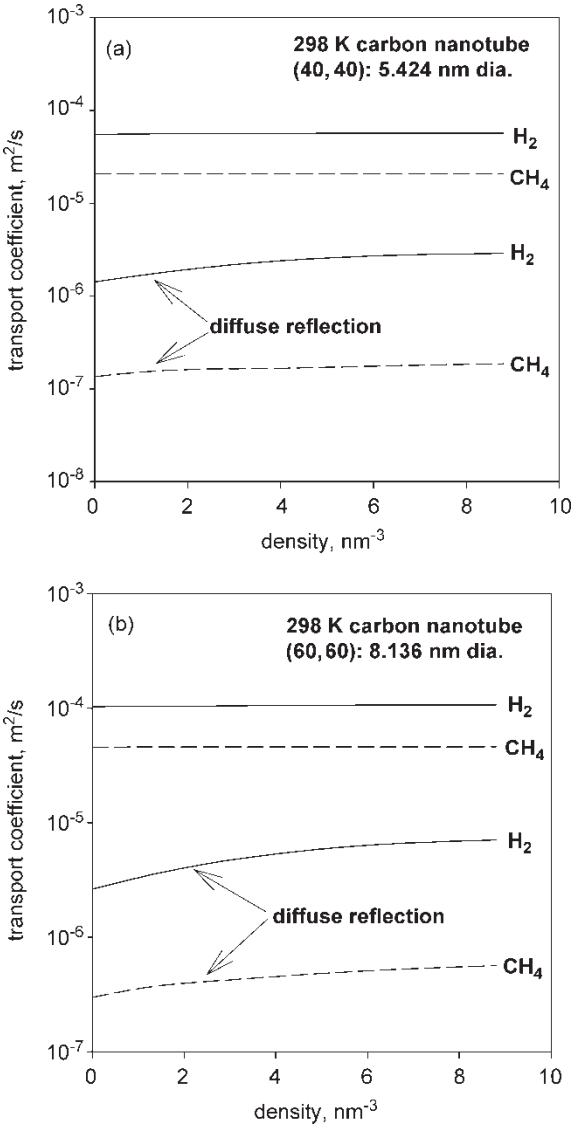

Figure 4. Corrected diffusion coefficients for CH_4 and H_2 adsorbed as single components at 298 K in (a) (40,40) SWNT's, and (b) (60,60) SWNT's, determined by equation (9). Upper curves are for the nanotubes using Maxwell coefficients appropriate for graphite, while lower set of curves are obtained for the case of diffuse wall reflection.

larger than for CH_4, and the physical reasons for this also apply to graphite. As a result, we estimated α to be 0.052 in the (40,40) and (60,60) SWNTs by simply multiplying our value for CH_4 by 4. In each case, we neglected any density dependence of α. Further the normalised density profile is assumed to be that corresponding to the Henry's law region.

Figure 4 depicts the predicted density variation of the transport coefficient of hydrogen and methane in the (40,40) and (60,60) nanotubes at 298 K, as well as the corresponding results for the case of diffuse reflection. As in the case of the smaller (10,10) nanotube the transport coefficients in the larger actual nanotubes are in the range of 10^{-5}–10^{-4}m^2/s, and almost two orders of magnitude larger than those attained if diffuse reflection occurs. Further, the difference in value of the coefficient between methane and hydrogen in the actual nanotubes is less than in the case of diffuse reflection, because of the higher value of α for hydrogen (for which the reflection is less specular).

The fraction of the net transport coefficient that arises from viscous contributions in (60,60) SWNTs, $[\alpha D_{\rm vis}(\hat{\rho})]/[(2-\alpha)D^{\rm DR}_{\rm diff}(\hat{\rho}=0)]$, is shown in figure 5. For both CH_4 and H_2 the effects of viscous transport are very small. Less than 0.6% of the net transport for CH_4 arises from viscous effects. For H_2 the effects are somewhat larger, but still contribute at most 4% of the overall transport. This is in sharp contrast to the result that would be observed if wall–fluid collisions occurred by diffuse reflection. The results for this limit are shown as the upper two curves in figure 5. The contribution of viscous effects diminishes as the nanotube diameter is reduced. For the (40,40) SWNT, the viscous contribution when the Maxwell coefficients above are used are less than 0.25% of the total for CH_4 and less than 2.6% for H_2.

These results would indicate that viscous flow is unlikely to be important in applications of nanotubes as materials for gas phase separation, even for tubes as large as 8 nm in diameter, and that surface slip provides the dominant mechanism of transport. While we have made the predictions for the larger (40,40) and (60,60) tubes based on reasonable assumptions regarding the Maxwell reflection coefficient and the density profile, as discussed above, we do not expect more precise computations to materially affect this conclusion because of the relative insignificance of the viscous contribution. Nevertheless, such studies are in progress and will be reported in a subsequent paper.

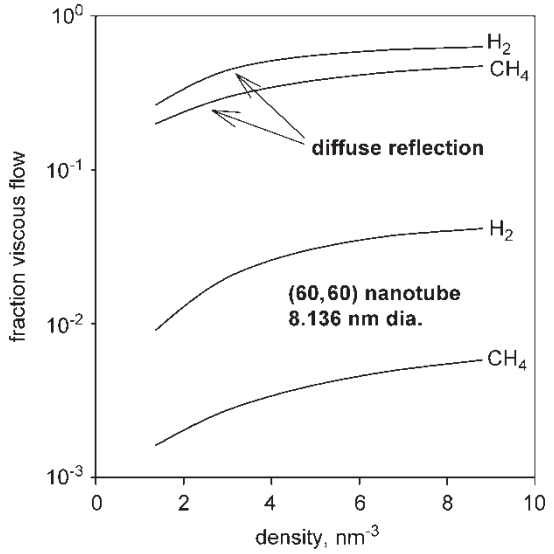

Figure 5. The fraction of the corrected diffusion coefficient arising from viscous contributions for CH_4 and H_2 in (60,60) SWNTs estimated using Maxwell coefficients appropriate for graphite (lower two curves) and using diffuse reflection (upper two curves).

5. Conclusions

Our analysis of the MD determined diffusion coefficients of hydrogen and methane in carbon nanotubes, based on theoretical estimates of the viscous contribution and of the diffusive contribution considering diffuse wall reflection, has yielded several interesting conclusions. In the first case very low values of the Maxwell coefficient are obtained for both gases, indicating nearly specular reflection, which reconciles very high reported values of transport coefficients in nanotubes. As expected the values of the Maxwell coefficient for hydrogen are larger than those for methane, due to the smaller size of the former, which makes it more sensitive to the atomic scale roughness of the nanotube surface. This less specular reflection of hydrogen also explains why its transport coefficient is comparable to that of methane, when under conditions of diffuse reflection the value for methane is about five times less than that for hydrogen, in a (10,10) nanotube. The reflection coefficient is also found to increase with density of the adsorbate, which is attributed to an effective roughening of the local potential energy landscape perceived by a molecule approaching the surface, due to intermolecular interactions among the fluid molecules. Further, the nearly specular reflection leads to dominance of the transport by the surface slip, with the viscous contribution being relatively small in comparison, even in tubes as large as 8.1 nm in diameter.

Acknowledgements

Work at CMU was partially supported by the NSF (CTS-0413027). Work at the University of Queensland has been supported by a grant from the Australian Research Council under the Discovery Scheme.

References

[1] C.N. Satterfield. *Heterogeneous Catalysis in Industrial Practice*, McGraw-Hill, New York (1991).
[2] R.T. Yang. *Gas Separation by Adsorption Processes*, Imperial College Press, London (1997).
[3] S.T. Hwang, K. Kammermeyer. *Membranes in Gas Separation*, Wiley, New York (1975).

[4] A.I. Skoulidas, D.M. Ackerman, J.K. Johnson, D.S. Sholl. Rapid transport of gases in carbon nanotubes. *Phys. Rev. Lett.*, **89**, 185901 (2002).
[5] D.M. Ackerman, A.I. Skoulidas, D.S. Sholl, J.K. Johnson. Diffusivities of Ar and Ne in carbon nanotubes. *Mol. Simul.*, **29**, 677 (2003).
[6] H. Chen, D.S. Sholl. Rapid diffusion of CH_4/H_2 mixtures in single-walled carbon nanotubes. *J. Am. Chem. Soc.*, **126**, 7778 (2004).
[7] V.P. Sokhan, D. Nicholson, N. Quirke. Fluid flow in nanopores: accurate boundary conditions for carbon nanotubes. *J. Chem. Phys.*, **117**, 8531 (2002).
[8] G. Arya, H-C. Chang, E.J. Maginn. Molecular simulation of wall slip: effect of pore morphology. *Mol. Simul.*, **29**, 697 (2003).
[9] R. Saito, G. Dresselhaus, M.S. Dresselhaus. *Physical Properties of Carbon Nanotubes*, Imperial College Press, London (1998).
[10] B.J. Hinds, N. Chopra, T. Rantell, R. Andrews, V. Gavalas, L.G. Bachas. Aligned multiwalled carbon nanotubes membranes. *Science*, **303**, 62 (2004).
[11] J. Kärger, D.M. Ruthven. *Diffusion in Zeolites and Other Microporous Solids*, Wiley, New York (1992).
[12] R. Krishna, J.A. Wesselingh. The Maxwell-Stefan approach to mass transfer. *Chem. Eng. Sci.*, **52**, 861 (1997).
[13] D. Nicholson, K. Travis. *Recent Advances in Gas Separation by Microporous Ceramic Membranes*, N.K. Kanellopoulos (Ed.), Elsevier, New York (2000).
[14] A.I. Skoulidas, D.S. Sholl. Transport diffusivities of CH_4, CF_4, He, Ne, Xe and SF_6 in silicalite from atomistic simulations. *J. Phys. Chem. B.*, **106**, 5058 (2002).
[15] G. Arya, H-C. Chang, E.J. Maginn. A critical comparison of equilibrium, non-equilibrium and boundary driven molecular dynamics techniques for studying transport in microporous materials. *J. Chem. Phys.*, **115**, 8112 (2001).
[16] T. Düren, L. Sarkisov, O.M. Yaghi, R.Q. Snurr. Design of new materials for methane storage. *Langmuir*, **20**, 2683 (2004).
[17] S.K. Bhatia, O. Jepps, D. Nicholson. Tractable molecular theory of transport of Lennard Jones fluids in nanopores. *J. Chem. Phys.*, **120**, 4472 (2004).
[18] M. Knudsen. *Kinetic Theory of Gases*, Methuen, London (1934).
[19] W.G. Pollard, R.D. Present. On gaseous self-diffusion in long capillaries. *Phys. Rev.*, **73**, 762 (1948).
[20] S.K. Bhatia, D. Nicholson. Hydrodynamic origin of diffusion in nanopores. *Phys. Rev. Lett.*, **90**, 016105 (2003).
[21] S.K. Bhatia, D. Nicholson. Molecular transport in nanopores. *J. Chem. Phys.*, **119**, 1719 (2003).
[22] I. Bitsanis, T.K. Vanderlick, M. Tirrell, H.T. Davis. A tractable molecular theory of flow in strongly inhomogeneous fluids. *J. Chem. Phys.*, **89**, 3152 (1988).
[23] O. Jepps, S.K. Bhatia, D. Searles. Modeling diffusion transport in slit pores. *J. Chem. Phys.*, **120**, 5396 (2004).
[24] T.H. Chung, M. Ajlan, L.L. Lee, K.E. Starling. Generalized multiparameter correlation for nonpolar and polar fluid transport properties. *Ind. Eng. Chem. Res.*, **27**, 671 (1988).
[25] R.L. Rowley, M.M. Painter. Diffusion and viscosity equations of state for a Lennard-Jones fluid obtained from molecular dynamics simulations. *Int. J. Thermophys.*, **18**, 1109 (1997).
[26] M.S. Zabaloy, J.M.V. Machado, E.A. Macedo. A study of Lennard-Jones equivalent analytical relationships for modeling viscosities. *Int. J. Thermophys.*, **22**, 829.
[27] O. Jepps, S.K. Bhatia, D. Searles. Wall mediated transport in confined spaces: exact theory for Lennard Jones fluids. *Phys. Rev. Lett.*, **91**, 0126102 (2003).
[28] S.K. Bhatia, D. Nicholson. Transport of Simple Fluids in nanopores: theory and simulation. *AICHEJ.*, submitted (2005).
[29] T. Duren, F.J. Keil, N.A. Seaton. Molecular simulation of adsorption and transport diffusion of model fluids in carbon nanotubes. *Mol. Phys.*, **100**, 3741 (2002).
[30] J.M.D. MacElroy, M.J. Boyle. Nonequilibrium molecular dynamics simulation of model carbon membrane separation of CH_4/H_2 mixtures. *Chem. Eng. J.*, **74**, 85 (1999).
[31] G. Arya, H.-C. Chang, E.J. Maginn. Knudsen diffusivity of a hard sphere in a rough slit pore. *Phys. Rev. Lett.*, 026102 (2003).
[32] V.P. Sokhan, D. Nicholson, N. Quirke. Fluid flow in nanopores: an examination of hydrodynamic boundary conditions. *J. Chem. Phys.*, **117**, 8531 (2002).